A Visibility and Total Suspended Dust Relationship

M.C. Baddock[1*], C.L. Strong[1], J.F. Leys[2], S.K. Heidenreich[2], E.K. Tews[3] and G.H. McTainsh[1]

[1]Atmospheric Environment Research Centre, Griffith School of Environment, Griffith University, Brisbane, Queensland, Australia 4111

[2]Office of Environment and Heritage, Science Division, Gunnedah, New South Wales, Australia 2380

[3]Australian Rivers Institute, Griffith School of Environment, Griffith University, Brisbane, Queensland, Australia 4111

*Corresponding author
Tel: +61 7 373 57645
Fax: +61 7 3735 4378
Email: m.baddock@griffith.edu.au

Abstract

This study reports findings on observed visibility reductions and associated concentrations of mineral dust from a detailed Australian case study. An understanding of the relationship between visibility and dust concentration is of considerable utility for wind erosion and aeolian dust research because it allows visibility data, which are available from thousands of weather observation stations worldwide, to be converted into dust concentrations. Until now, this application of visibility data for wind erosion/dust studies has been constrained by the scarcity of direct measurements of co-incident dust concentration and visibility measurements. While dust concentrations are available from high volume air samplers, these time-averaged data cannot be directly correlated with instantaneous visibility records from meteorological observations. This study presents a new method for deriving instantaneous values of total suspended dust from time averaged (filter-based) samples, through reference to high resolution PM_{10} data. The development and testing of the model is presented here as well as a discussion of the derived expression in relation to other visibility-dust concentration predictive curves. The current study is significant because the visibility-dust concentration relationship produced is based on visibility observations made 10-100 km from the dust sources. This distance from source makes the derived relationship appropriate for a greater number of visibility recording stations than widely-used previous relationships based on observations made directly at eroding sources. Testing of the new formula performance against observed total suspended dust concentrations demonstrates that the model predicts dust concentration relatively well (r^2 = 0.6) from visibility. When considered alongside previous studies, the new relationship fits into the continuum of visibility-dust concentration outcomes existing for increasing distance-from-source. This highlights the important influence that distance to source has on the visibility-dust concentration relationship.

Keywords: duststorm; sandstorm; air quality; PM10; aerosols; TSP

1. Introduction

The visibility distance at the time of observation is a commonly reported atmospheric variable in meteorological data. The presence of smoke, pollution, moisture and suspended mineral dust in the atmosphere can all result in a reduction in visibility. The impact that dust has on visibility is a chief cause of the transport disruptions caused by these aeolian phenomena (Baddock et al., 2013; Tozer and Leys, 2013). For research into aeolian dust, the degree of visibility reduction associated with dust-related weather codes has provided fundamental information on the spatio-temporal characteristics of dust activity. Before the advent of satellite remote sensing, visibility was the dominant variable used in mapping the distribution of wind erosion and dust activity (Orgill and Sehmel, 1976; Middleton et al., 1986; McTainsh and Pitblado, 1987; Goudie and Middleton, 1992).

Visibility has been widely used in dust studies because these basic data are readily available from thousands of observation stations in the World Meteorological Organisation (WMO) network, and are often available for long time series. Values of the concentration of dust in the atmosphere however represent a more process relevant and precisely quantifiable measure of mineral dust loading than visibility. For instance, dust concentration is the form by which off-site air quality is measured and regulated, such as in maximum concentration for dust particles of all sizes, TSD (Total Suspended Dust), or size-selective e.g., PM_{10} (particles <10 μm) (e.g., Stetler and Saxton, 1996; Neff et al., 2013).

Estimates of dust concentration can be derived from visibility measurements, and several empirical relationships that relate concentration to visibility have previously been put forward (e.g., Chepil and Woodruff, 1957; Patterson and Gillette, 1977; Ben Mohamed and Frangi, 1986; D'Almeida, 1986; Chung et al., 2003; Wang et al., 2008). Such visibility-based estimates of dust concentration have numerous applications in; the mapping of wind erosion (McTainsh et al., 2008; O'Loingsigh, 2014), the 'ground truthing' of remote sensing (Wang and Christopher, 2003; Guo et al., 2009), air quality assessments (Ozer et al., 2006; Dagsson-Waldhauserova et al., 2013), the validation of dust activity modelling (Shao et al., 2003; 2007), the estimation of peak loads of large dust storms (Raupach et al., 1994; Chung et al., 2003; McTainsh et al., 2005; Leys et al., 2011) and for better understanding the effects of suspended mineral aerosols on the radiative budget (e.g., Sokolik et al., 2001; Satheesh and Moorthy, 2005).

The various empirical expressions that relate visibility and dust concentration have been found to differ between studies (Patterson and Gillette, 1977; Ben Mohamed and Frangi, 1986; Dayan et al., 2007; Shao et al., 2007; Wang et al., 2008). For such expressions to be useful in dust-atmospheric studies, it is important that this variability be understood. Furthermore, so that accurate estimates of dust concentration can be produced from visibility, it is also important that the most appropriate expression be applied for a given visibility observation location. The need to understand the relationship between visibility and dust concentration as part of wind erosion research has long been recognised (e.g., Ette and Olorode, 1988; Ackerman and Cox, 1989; Shao et al., 2003). In particular, two classic studies in the United States, those of Chepil and Woodruff (1957) and Patterson and Gillette (1977) used empirical fits of observed data to describe the relationship

$$C_m = A/V^{\gamma} \qquad (1)$$

with

$$A = C_m V \qquad (2)$$

where C_m is total mass concentration, A is a term related to the effects on extinction due to particle size distribution, γ a constant and V is observed visibility. These studies demonstrate the suitability of the power relationship in describing the relationship between visibility and dust concentration. Patterson and Gillette (1977) noted the variety in the values of constant terms put forward to relate concentration and visibility. They attributed the lack of a single applicable term to variations in dust particle size distributions (PSD) between both dust events and study areas. PSDs can be highly variable between wind erosion episodes, and are controlled chiefly by source soil characteristics, wind erosivity and the distance of observation point from the eroding source (El-Fandy, 1953, Chepil and Woodruff, 1957).

It is noteworthy that both the Chepil and Woodruff (1957) and Patterson and Gillette (1977) studies were based on visibility and dust concentration measurements made at, or very close to, eroding sources. This constrains the application of their visibility and dust concentration functions because worldwide, the most readily available source of visibility data is from WMO meteorological stations which are impacted by dust, but are not located directly at the eroding source. An expression describing the visibility and dust concentration relationship at a greater distance from source will therefore be more appropriate for these locations. Following terminology from the transport distance model of Tsoar and Pye (1987), dust within a few kilometres from its source can be termed local, while >10 km dust can be regarded as regional (see also Cattle et al., 2009).

The aim of this study was to produce a relationship between visibility and total suspended dust concentration for dust events observed at a regional scale (10-100 km) from source. A new method is presented here for obtaining instantaneous dust concentrations from time-averaged data, to allow their correlation with instantaneous visibility observations.

2. Methods

2.1 Background to methods

The most reliable source of near-surface dust concentration data is field sampling using active samplers, such as vacuum pump-based devices (e.g., Nickling and Gillies, 1993; Nickling et al. 1999), or from networks of high volume samplers (HVS) (Leys et al., 2008). Such equipment however is costly, labour intensive to operate and largely impractical for widespread spatial monitoring of dust, especially in remote areas. A more widely applicable approach for wind erosion monitoring involves the use of DustTrak® (TSI, St. Paul, MN, USA) samplers (Leys et al*.,* 2008). DustTrak instruments provide real time dust concentrations, but only for particulates with an aerodynamic size of <10 µm (PM_{10}). This size selectivity makes such instruments suitable for monitoring air pollution and the associated effects that fine particles have on human health. While PM_{10} is being successfully used for wind erosion mapping (e.g., Wang et al., 2008), wind erosion events also entrain coarser particles than this size. As a result, PM_{10} does not fully characterise all dust events, or describe the full size range of suspended particles contributing to atmospheric mass loadings (Tsoar and Pye, 1987; Lawrence and Neff, 2009; Neff et al., 2013). It is preferable therefore for measurements of dust concentration for a given dust event to be calculated from the entire range of particle sizes present.

High volume samplers (HVS) collect the total range of particles in the air, but as the resultant dust concentration is time-integrated over the total sampling period for which the HVS was operating (generally 24 h), these time-averaged data have a poor relationship with time-averaged visibility. The focus of the current study is to use the high resolution time series of PM_{10} dust concentration measured with a DustTrak (C_{DT}) to calculate the equivalent total dust concentration measured with a co-located HVS (C_{HVS}) for a point in time (C_{HVSi}), which can then be correlated with the concurrent visibility. The resultant relationship is referred to from here on as the Visibility-Total Suspended Dust (V-TSD) model.

2.2 Site and sampling details

A HVS and a DustTrak instrument, operated by the New South Wales Office of Environment and Heritage (OEH) and Griffith University, provide two forms of dust concentration data at Buronga, New South Wales (34.17°S, 142.20°W). The HVS at this site constitutes the longest rural record of dust concentration in Australia, monitoring dust in the intensively cultivated Mallee region for over 24 years (Leys et al., 2008). For dust events, the HVS collects the full range of suspended particles on glass fibre filter papers (Whatman GF/A with nominal pore size of 1.6 μm) using a sampling flow rate of about 0·7 m^3 min^{-1}. The record of HVS dust event concentration data from Buronga was examined for the years 2004 – 2007.

Determination of dust concentration from the HVS is in part governed by the duration that each filter sampled for. As filter changing is a manual operation, the sampling time varied for each filter (20-75 hours). This time period introduces the chance of multiple dust events becoming sampled. In conjunction with the HVS filter data, 5-minute PM_{10} data from the DustTrak at Buronga were also used in order to measure the timing and duration of the dust events.

The dust concentration data gathered at Buronga were correlated with visibility data from Mildura, Victoria as the nearest Australian Bureau of Meteorology (BoM) station, located 12 km to the south-west of Buronga. Visibility data from Mildura came from two datasets; the regular 3-hourly synoptic observation (Vis_{synop}) (excluding the midnight 0000 reading) and irregular A37 visibility recordings (Vis_{A37}), which have a 5 to 30-minute frequency when available. A37 reports augment the synoptic record and are typically recorded during notable weather phenomena such as dust events.

Whilst it would have been preferable to have the concentration sampling sited at the same location as the BoM visibility observation, for practical reasons this was not possible. The siting of instruments and the observer in different locations creates some challenges and these were taken into account by the method used for comparing visibility and dust concentration.

2.3. Deriving instantaneous dust concentration from HVS data

From the HVS filters obtained at Buronga during 2004-2007, a total of 13 filters was used to create a high quality dataset comprising 83 discrete dust concentrations. The selection criteria producing the 13 filters included: i) TSD load >100 µg/m3 and filter run time between 18 and 30 hours, ii) a continuous 5-minute PM_{10} concentration record existed for the HVS sampling period, iii) the availability of high temporal resolution A37 visibility observations for the dust event and iv) wind direction during the event from the south west, to ensure that dust observed at Mildura was measured at Buronga.

Given that the DustTrak is limited to recording the PM_{10} fraction, the ratio between PM_{10}/TSD was determined for each dust event in order to relate the high frequency PM_{10} concentration to TSD. Calculation of this ratio involves two assumptions; i) that the PM_{10} dust concentration time series is the same as the TSD time series, and the only difference between the measurements is the particle size limitation of the PM_{10} measurements, ii) that the PM_{10} to TSD ratio is constant over the HVS sample period t=0 to t=T. Accepting these conditions, equation 3 defines how the PM_{10}/TSD ratio (a) relates the DustTrak and HVS concentrations

$$C_{DT_t} = a * C_{HV_t} \qquad (3)$$

where C_{DT_t} is PM_{10} concentration from DustTrak, C_{HV_t} is TSD concentration from HVS, and a is the ratio between the two. This ratio was determined for each HVS filter paper used, or in other words, for each dust event examined.

The total mass *m* collected on the filter paper for any given time interval *t=0* to *t=T* is

$$m = \int_{t=0}^{t=T} C_{HV_t} * \frac{dV}{dt} * dt \qquad (4).$$

Because the volume of air flow passing through the filter can be regarded as a constant for each sampling event ($\dot{V} = dV/dt$), re-arranging equations 3 and 4 produces

$$m = \frac{\dot{V}}{a} * \int_{t=0}^{t=T} C_{DT_t} * dt \qquad (5).$$

From the total mass on the filter for the sampling period, the total air volume sampled, and the time-averaged PM_{10} concentration of the DustTrak ($\bar{C}_{DT_t}$) for the same period, the value of *a* can be determined through

$$\bar{C}_{DT_t} = a * \bar{C}_{HV_t} \qquad (6)$$

re-arranged to

$$a = \frac{C_{DT_t}}{m_{HV}/V_{HV}} \qquad (7).$$

As the object of the study was to relate visibility to dust concentration, an instantaneous value of TSD concentration at time (C_{HV_t} at time *i*) was required. For this, equation 8 was applied

$$C_{HV_i} = \frac{C_{DT_i}}{a} \qquad (8).$$

To obtain C_{HV_i}, first, the measured PM_{10} concentration C_{DT_i} was obtained for *i* when an A37 visibility reading existed. One issue with the split-site sampling and the distance between Mildura and Buronga is the small time difference in the onset of dust between the two locations (Figure 1). As this effectively represents a time lag between the sites, the time difference was calculated and applied to the lagging station to ensure that A37 visibilities and PM_{10} data corresponded with one another. For instance, in Figure 1, the drop in visibility marking the event onset occurred at 18:13 at Mildura, when windspeed was 42 km/h and wind direction 220°. At Buronga, downwind of Mildura and to the NE, the peak PM_{10} concentration was 11 minutes later, an acceptable time lag given the Mildura wind data and the 12 km distance between the sites. Per equation 8, the PM_{10} concentration at *i* was divided by the PM_{10}/TSD ratio (*a*) to yield an instantaneous TSD concentration for the time of the visibility reading.

>>Figure 1 here

2.4 Testing the V-TSD model

In order to validate the V-TSD expression, a comparison was made between values of dust concentration estimated from the model and those directly measured by the HVS. From the HVS filters obtained at Buronga during 2002 and 2003, a total of 22 filters was used as a test database, with each one representing an individual dust event. The use of this time period, which was prior to the years used to develop the V-TSD model, ensured the test dataset was independent of that used to formulate the model. To incorporate a range of dust concentrations in the testing (i.e., different dust event intensities), of the 22 events, four filters were randomly chosen from events with C_{HVS} >300 μg/m^3 to represent relatively intense dust conditions, seven filters for moderate dust concentration (100-300 μg/m^3) and eleven filters with <100 μg/m^3.

For each test event, the Vis_{synop} values during the HVS sampling period were used to determine visibility. Given that C_{HVS} represents the dust concentration over the extended period that the HVS sampled, multiple three-hourly Vis_{synop} values existed for each dust event. To account for this, the V-TSD modelled dust concentration was calculated for an event by substituting each visibility into the V-TSD model and then weighting the result by the time period that the visibility represented. This was achieved through multiplication of the estimated concentration by the time interval (e.g., three hours). The time-weighted concentration values were summed and divided by total event duration to produce the modelled concentration (C_{VTSD}).

3. Results

The extended duration of individual dust events typically provided multiple high-frequency A37 visibilities at different times throughout each event. Equation 8 could therefore be applied to a range of visibilities and therefore dust concentrations (n = 83) from the 13 events of 2004-2007. Best fitting this data produced the V-TSD model (Figure 2) represented by the relationship

$$C_{VTSD} = 4050 * Vis^{-1.016} \qquad (9)$$

where C_{VTSD} is total suspended dust concentration (μg/m^3) and *Vis* is visibility (km). The power form for the expression was adopted because comparable earlier studies produced expressions of this form, also with power functions close to 1 (Chepil and Woodruff, 1957; Patterson and Gillette, 1977; Wang et al., 2008), and the r^2 = 0.79 of equation 9 reveals a relatively strong correlation.

>>Figure 2 here

Section 2.4 detailed how a dataset was produced in order to test the predictive ability of the V-TSD model. When dust concentrations calculated by equation 9 (C_{VTSD}) were plotted against the measured HVS dust concentration (C_{HVS}) for 22 independent dust events from 2002-2003, a positive linear fit resulted with an r^2 = 0.60 (Figure 3).

>>Figure 3 here

4. Discussion

4.1 The V-TSD model

The aim of this study was to examine the relationship between TSD concentration and visibility for the Mildura/Buronga location. Although the correlation between TSD and visibility is relatively strong, in some sections of the plot the strength of the relationship is weaker (Figure 2). Between 3 and 6 km visibility, concentrations generated by the V-TSD model were greater than the line of best fit. This is most likely a consequence of overestimation of visibility by observers for this range of distance, and is exacerbated by the relatively few observations at visibilities between 1 and 3 km. For visibility observations of 7 km and above, dust concentrations were variable, but typically under 1000 µg/m^3. At these distances, the variation in the recorded concentration values for a given visibility must partly reflect the subjectivity of visibility estimation at such range in conditions with reduced dust loading.

The V-TSD model is based on the consideration that it is the complete particle size range of suspended dust that exerts a fuller influence on visibility (El-Fandy, 1953). However, as the DustTrak instrument also provided direct measurements of PM_{10} concentration, a useful comparison can be made between the relationship of PM_{10} concentration with visibility, and that of TSD from Figure 2. Using instantaneous PM_{10} concentrations in place of the modeled TSD values, the weaker correlation with visibility that the size selective dust concentration results in, compared to the full particle size range, is evident (Figure 4). In fact, the contribution that large (>PM_{10}) dust particles make to total dust concentrations in the Colorado Plateau region of the U.S. has recently been demonstrated by Neff et al. (2013). Given the relative prevalence of PM_{10} monitoring devices however, for instance, as part of air quality monitoring networks, the relationship between visibility and the concentration of dust limited to PM_{10} size is still of appreciable utility for wind erosion studies (Chung et al., 2003; Dayan et al., 2007; Wang et al., 2008; Leys et al., 2011).

>>Figure 4 here

4.2 Comparison of the V-TSD model with other studies

Patterson and Gillette (1977) commented that expressions for estimating dust concentration from visibility would vary between studies, explaining that the relative concentration of large particles exerts a strong influence on the visibility-dust concentration relationship. They stated that different soil conditions as well as the distance that the dusts had been transported would control the proportion of large particles present to affect visibility. Further insights into the nature of these controls upon the visibility-dust concentration relationship can be gained by comparing the curves of previous studies with the V-TSD relationship of equation 9 (Figure 5).

>>Figure 5 here

To explain the divergence between Chepil and Woodruff's (1957) expression and that of their own work, Patterson and Gillette (1977) postulated that different soil conditions between the studies produced different dust PSDs. They suggested that the drought conditions during Chepil and Woodruff's (1957) monitoring period (1954 – 1955) produced more erodible soils which resulted in increased dust particle size. This in turn produced higher dust concentrations for a given level of visibility, an effect evident in the displacement of the Chepil and Woodruff line in Figure 5. Patterson and Gillette also correctly assert that the difference in these empirical relationships was not due to distance from source because sampling in both studies was conducted very close to, or directly at, the eroding surfaces. Conversely, they show that the lower dust concentrations measured in the study by Bertrand et al. (1974) arose because the dusts were sampled approximately 2000 km from source.

While the particle size characteristics of dust have been found to relate to the particle size of the source soil (e.g. Gillette and Walker, 1977; Alfaro and Gomes, 2001) the influence that the parent soil has on the PSD of dust is strongest near to source, directly above the wind-eroded surface from where the dust is entrained (Tsoar and Pye, 1987). Furthermore, the entraining wind strength has been argued to affect the PSD of dust, with the influence of this factor again dominant near to source (e.g., Gillette and Walker, 1977), though this theory is not without challenge (see Kok, 2011). For both these factors, their influence on dust PSD would be greatest closer to entrainment because with downwind transport, larger particles preferentially settle out so differences in PSD will be reduced with distance from source (Pye, 1987).

In the present study, it is significant that the dust sampling at Mildura/Buronga was not conducted immediately 'at source'. Wind erosion mapping based on meteorological observations of dust show that the cultivated sandy soils of the Mallee region 10-100 km SW of the Mildura/Buronga site is the main source region for the examined dust events (McTainsh and Pitblado, 1987). At this distance, the PSD of sampled dust would be relatively finer than at-source due to coarser particles settling out closer to source (Tsoar and Pye, 1987). As finer particles have a greater relative influence on visibility impairment than on mass concentration, the reduction of visibility by a given dust concentration is greater at a point further from source. The differences between our V-TSD expression and those of Chepil and Woodruff (1957) and Patterson and Gillette (1977) therefore probably result more from the effect of distance-from-source, than parent soil particle size or eroding wind conditions (Figure 5). A similar result is also seen in the work of Shao et al. (2003; also Shao and Wang, 2003). In their study, the effects of distance from source were accommodated by using two expressions of the dust concentration to visibility relationship; one for cases above a threshold visibility of 3.5 km (assumed to be distant dusts) and the other for below 3.5km visibility (local dusts).

Distance from source effects may also be demonstrated by values of *A* (equation 2), as the term used to characterise the effects of the suspended PSD on optical extinction. Patterson and Gillette (1977) explain that *A* should be lower for observations made at greater distance from source, again owing to the reduced contribution to visibility attenuation from larger sized particles when further from source. The findings here show good agreement with the range of *A* values presented by Patterson and Gillette. The *A* outcomes for measurements predominantly at eroding field sources were 5.6×10^{-2} g m^{-3} km in Chepil and Woodruff (1957) and 2.0×10^{-2} g m^{-3} km for Patterson and

Gillette (1977). The lower average of A (4.6×10^{-3} g m^{-3} km) from the current study of regional erosion reflects the fact that observations were made at a greater distance from source (< ~100 km). In the case of distantly sourced dust, Patterson and Gillette (1977) estimated $A = 1.4 \times 10^{-3}$ g m^{-3} km for observations made approximately 2000 km from source using data of Bertrand et al. (1974). This result further reinforces the significance of distance from source for expressing the effect of dust on visibility.

By adding our new visibility-dust concentration curve developed for regional dusts (i.e., dust transported and observed some 10-100 km from source) to two previous visibility-dust concentration curves from at-source (Figure 5), it is now possible to more accurately estimate dust concentration using the visibility data from a much larger number of WMO stations. Our V-TSD relationship applies to the greater proportion of stations located in regions experiencing dust transport, but not located directly at the source of dust. By enhancing our capability to estimate dust concentration away from source areas, improved concentration estimates will allow for better and more complete; mapping of wind erosion (O'Loingsigh et al., 2014), comparison of ground data with remote sensing aerosol products (e.g. MODIS Deep Blue (Ginoux et al., 2012)), validation of dust emission models, and, the estimation of peak loads of large dust storms, within the region an order of 10-100 km downwind from source.

In addition, the methodology demonstrated here provides a means of further expanding the suite of visibility-dust concentration curves by using HVS, DustTrak and visibility data from WMO stations in other wind erosion settings. For example, medium distance dust concentrations could be estimated without the need to conduct dedicated field experiments of the type originally carried out by Patterson and Gillette (1977).

5. Conclusion

This study is an outcome of an ongoing, long term, synergistic dust monitoring program in rural New South Wales, Australia (Leys et al., 2008; McTainsh et al., 2008). The study applies a novel methodology to data from high volume sampler and DustTrak dust monitoring devices to derive instantaneous values of total suspended dust concentration from time-averaged values. By relating high frequency meteorological visibility reports to the derived at-a-time concentrations, an empirical relationship between observed visibility and measured dust concentration was produced. Whereas previous studies were based on field experiments dedicated to exploring the relationship between visibility and dust concentration, the current study presents an innovative way of utilising existing datasets to quantify this relationship.

The new model for visibility and dust concentration from the Mildura/Buronga location demonstrates the effect that distance from source has on the nature of the relationship. Prominent previous studies produced expressions based on observations made at, or very close to, the eroding soil source. The current study, by using visibility and concentration measurements made further from source (10-100 km) demonstrates the influence of particle size, in this case, reduced particle size of the dust as a result of this regional distance from source. The new visibility-dust concentration expression is therefore more appropriate to visibility data from those observer stations regional to source areas. This makes the expression applicable to a larger number of WMO stations.

Acknowledgements

The authors extend thanks to Terry Koen for statistical advice and Michael Case (both New South Wales Office of Environment and Heritage) for changing hundreds of HVS filter papers, obtaining manually recorded visibility records from the BoM and maintaining the DustTrak. We also thank the input of the editor regarding an early draft of the manuscript, and the constructive comments of two anonymous reviewers.

References

Ackerman, S.A., Cox, S.K., 1989. Surface weather observations of atmospheric dust over the Southwest Summer Monsoon Region. Meteorology and Atmospheric Physics 41, 19-34.

Alfaro, S.C., Gomes, L., 2001. Modeling mineral aerosol production by wind erosion: emission intensities and aerosol size distributions in source areas. Journal of Geophysical Research 106, D16, 18075-18084.

Baddock, M.C., Strong, C.L., Murray, P.S., McTainsh, G.H., 2013. Aeolian dust as a transport hazard. Atmospheric Environment 71, 7-14.

Ben Mohamed, A., Frangi, J.-P., 1986. Results from ground-based monitoring of spectral aerosol optical thickness and horizontal extinction: some specific characteristics of dusty Sahelian atmospheres. Journal of Climate and Applied Meteorology 25, 1807-1815.

Bertrand, J., Baudet, J., Drochon, A., 1974. Importance des aerosols naturels en Afrique de L'ouest. Journal de Recherches Atmospheriques 8, 845-860.

Cattle, S.R., McTainsh, G.H., Elias, S., 2009. Æolian dust deposition rates, particle-sizes and contributions to soils along a transect in semi-arid New South Wales, Australia. Sedimentology 56, 765-783.

Chepil, W.S., Woodruff, N.P., 1957. Sedimentary characteristics of Dust Storms: II. Visibility and dust Concentration. American Journal of Science 255, 104-114.

Chung, Y.S., Kim, H.S., Park, K.H., Jhun, J.G., Chen, S.J., 2003. Atmospheric loadings, concentrations and visibility associated with sandstorms: satellite and meteorological analysis. Water, Air, and Soil Pollution: Focus 3, 21-40.

Dagsson-Waldhauserova, P., Arnalds, O., Olafsson, H., 2013. Long-term frequency and characteristics of dust storm events in Northeast Iceland (1949-2011). Atmospheric Environment 77, 117-127.

D'Almeida, G.A., 1986. A model for Saharan dust transport. Journal of Climate and Applied Meteorology 25, 903-916.

Dayan, U., Ziv, B., Shoob, T., Enzel, Y., 2008. Suspended dust over southeastern Mediterranean and its relation to atmospheric circulations. International Journal of Climatology 28, 915-924.

El-Fandy, M.G., 1953. On the physics of dust atmospheres. Quarterly Journal of the Royal Meteorological Society 79, 284-287.

Ette, A.I.I., Olorode, D.O., 1988. The effects of the Harmattan dust on air conductivity and visibility at Ibadan, Nigeria. Atmospheric Environment 22, 2625-2627.

Gillette, D.A., Walker, T.R., 1977. Characteristics of airborne particles produced by wind erosion of sandy soil, High Plains of West Texas. Soil Science 123, 97-110.

Ginoux, P., Prospero, J.M., Gill, T.E., Hsu, N.C., Zhao, M., 2012. Global-scale attribution of anthropogenic and natural dust sources and their emission rates based on MODIS Deep Blue Aerosol products. Reviews of Geophysics 50, RG3005.

Goudie, A.S., Middleton, N.J., 1992. The changing frequency of dust storms through time. Climatic Change 20, 197-225.

Guo, J.-P., Zhang, X.-Y., Che, H.-Z., Gong, S.-L., An, X., Cao, C.-X., Guang, J., Zhang, H., Wang, Y.-Q., Zhang, X.-C., Xue, M., Li, X.-W., 2009. Correlation between PM concentrations and aerosol optical depth in eastern China. Atmospheric Environment 43, 5876-5886.

Kok, J.F., 2011. Does the size distribution of mineral dust aerosols depend on the wind speed at emission? Atmospheric Chemistry and Physics 11, 10149-10156.

Lawrence, C.R., Neff, J.C., 2009. The contemporary physical and chemical flux of aeolian dust: a synthesis of direct measurements of dust deposition. Chemical Geology 267, 46-63.

Leys, J., McTainsh, G., Strong, C., Heidenreich, S., Biesaga, K., 2008. DustWatch: using community networks to improve wind erosion monitoring in Australia. Earth Surface Processes and Landforms 33, 1912-1926.

Leys, J.F., Heidenreich, S.K., Strong, C.L., McTainsh, G.H., Quigley, S., 2011. PM_{10} concentrations and mass transport during "Red Dawn" – Sydney 23 September 2009. Aeolian Research 3, 327-342.

McTainsh, G.H., Pitblado, J.R., 1987. Dust storms and related phenomena measured from meteorological records in Australia. Earth Surface Processes and Landforms 12, 415–424.

McTainsh, G., Chan, Y.-C., McGowan, H., Leys, J., Tews, K., 2005. The 23rd October 2002 dust storm in eastern Australia: characteristics and meteorological conditions. Atmospheric Environment 39, 1227–1236

McTainsh, G., Leys, J., Tews, K., Strong, C., 2008. Dust Storm Index to Dust Concentration: Developing a new measure of wind erosion for national and state scale monitoring. Final Report and User Guide. Griffith University, Brisbane, pp. 32.

Middleton, N. J., Goudie, A.S., Wells, G.L., 1986. The frequency and source areas of dust storms. In *Aeolian Geomorphology*, edited by W. G. Nickling, pp. 237–259, Allen & Unwin, Boston.

Neff, J.C., Reynolds, R.L., Munson, S.M., Fernandez, D., Belnap, J., 2013. The role of dust storms in total atmospheric particle concentrations at two sites in the western U.S. Journal of Geophysical Research 118, 11201-11212.

Nickling, W.G., Gillies, J.A., 1993. Dust emission and transport in Mali, West Africa. Sedimentology 40, 859-868.

Nickling, W.G., McTainsh, G.H., Leys, J.E., 1999. Dust emissions from the Channel Country of western Queensland, Australia. Zeitschrift fur Geomorphologie N.F. 116, 1-17.

Orgill, M.M., Sehmel, G.A., 1976. Frequency and diurnal variations of dust storms in the contiguous USA. Atmospheric Environment 10, 813-825.

Ozer, P., Laghdaf, M.B.O.M., Lemine, S.O.M., Gassani, J., 2006. Estimation of air quality degradation due to Saharan dust at Nouakchott, Mauritania, from horizontal visibility data. Water Air and Soil Pollution 178, 79-87.

Patterson, E.M., Gillette, D.A., 1977. Measurements of visibility vs mass of airborne soil particles. Atmospheric Environment 11, 193-196.

Pye, K., 1987. Aeolian Dust and Dust Deposits. Academic Press, London.

Raupach, M.R., McTainsh, G.H., Leys, J.F., 1994. Estimates of dust mass in recent major dust storms. Australian Journal of Soil and Water Conservation 7, 20–24.

Satheesh, S. K., Moorthy, K. K., 2005. Radiative effects of natural aerosols. Atmospheric Environment 39, 2089−2110.

Shao, Y., Wang, J., 2003. A climatology of northeast Asian dust events. Meteorologische Zeitschrift 12, 187-196.

Shao, Y., Yang, Y., Wang, J., Song, Z., Leslie, L.M., Dong, C., Zhang, Z., Lin, Z., Kanai, Y., Yabuki, S., Chun, Y., 2003. Northeastern Asian dust: Real-time numerical prediction and validation. Journal of Geophysical Research 108, D22, 4691.

Shao, Y., Leys, J.F., McTainsh, G.H., Tews, K., 2007. Numerical simulation of the October 2002 dust event in Australia. Journal of Geophysical Research 112, D08207.

Sokolik, I. N., Winker, D.M., Bergametti, G., Gillette, D.A., Carmichael, G., Kaufman, Y.G., Gomes, L., Schuetz, L., Penner, J.E., 2001. Introduction to special section: Outstanding problems in quantifying the radiative impacts of mineral dust. Journal of Geophysical Research 106, 18015–18027.

Stetler, L.E., Saxton, K.E., 1996. Wind erosion and PM_{10} emissions from agricultural fields on the Columbia Plateau. Earth Surface Processes and Landforms 21, 673-685.

Tsoar, H., Pye, K., 1987. Dust transport and the question of desert loess formation. Sedimentology 34, 139-153.

Tozer, P. R., Leys, J., 2013. Dust storms - What do they really cost? The Rangeland Journal 35, 131-142.

Wang, J., Christopher, S.A., 2003. Intercomparison between satellite-derived aerosol
optical thickness and PM2.5 mass: implications for air quality studies. Geophysical Research Letters 30, 2095.

Wang, Y.Q., Zhang, X.Y., Gong, S.L., Zhou, C.H., Hu, X.Q., Liu, H.L., Niu, T., Yang, Y.Q., 2008. Surface observation of sand and dust storm in East Asia and its application to CUACE/Dust. Atmospheric Chemistry and Physics 8, 545-553.

Figure Captions

Figure 1: The 5-minute PM_{10} dust concentration record from the DustTrak at Buronga and visibility (A37 records) at Mildura for the dust event of December 12^{th} 2005. Note inverted visibility on secondary vertical axis. Dashed lines mark the onset of the event as detected by each monitoring technique. The displacement of the plots arises because the dust event reached Mildura before Buronga (see Section 2.3).

Figure 2: The relationship between visibility and total suspended dust for the Mildura/Buronga sampling location, expressed as the V-TSD model (n = 83).

Figure 3: Measured total suspended dust concentration by HVS (C_{HVS}) and modelled total suspended dust concentration by V-TSD (C_{VTSD}) for 22 dust events experienced at Buronga, NSW during 2002-03 (see Section 2.4).

Figure 4: The relationship between visibility and PM_{10} dust for the Mildura/Buronga sampling location (n = 83).

Figure 5: Comparison between the V-TSD model and other selected expressions relating dust concentration and visibility, from Chepil and Woodruff (1957) (C&W) and Patterson and Gillette (1977) (P&G).

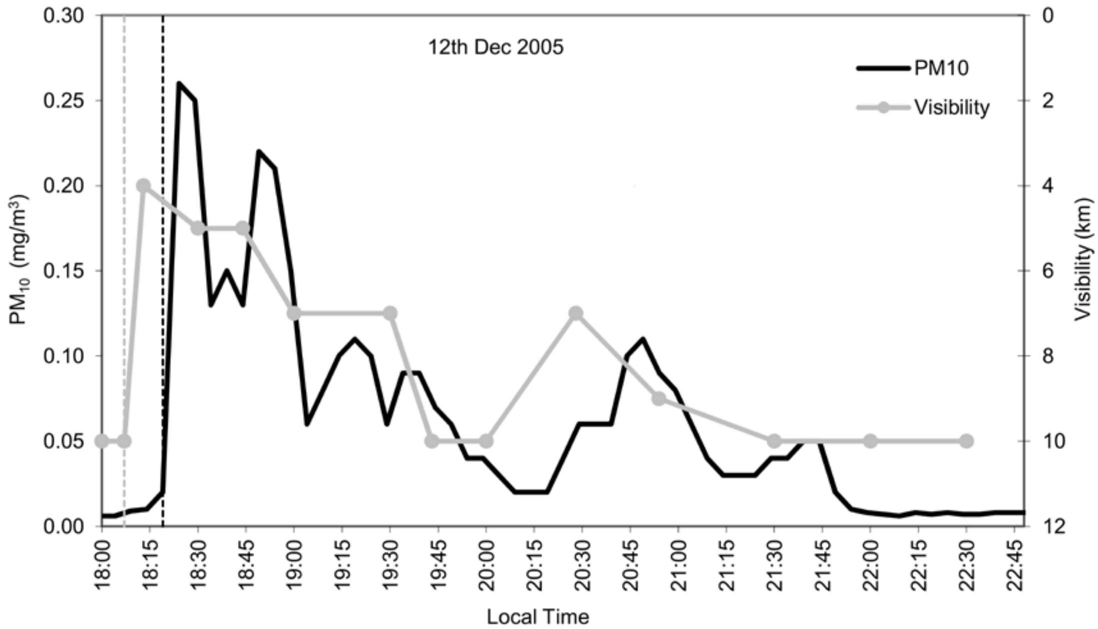

12th Dec 2005
PM10
Visibility
PM$_{10}$ (mg/m^3)
Visibility (km)
Local Time
0.30
0.25
0.20
0.15
0.10
0.05
0.00
0
2
4
6
8
10
12
18:00
18:15
18:30
18:45
19:00
19:15
19:30
19:45
20:00
20:15
20:30
20:45
21:00
21:15
21:30
21:45
22:00
22:15
22:30
22:45

Figure 1

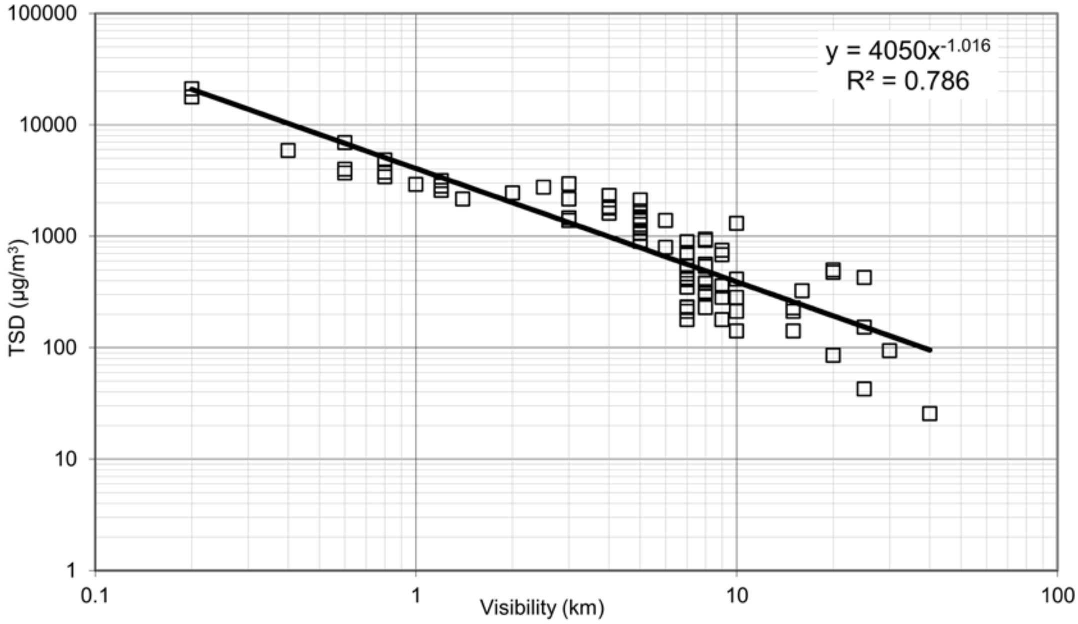
100000
10000
1000
100
10
1
TSD (µg/m3)
0.1
1
10
100
Visibility (km)
y = 4050x-1.016
R² = 0.786

Figure 2

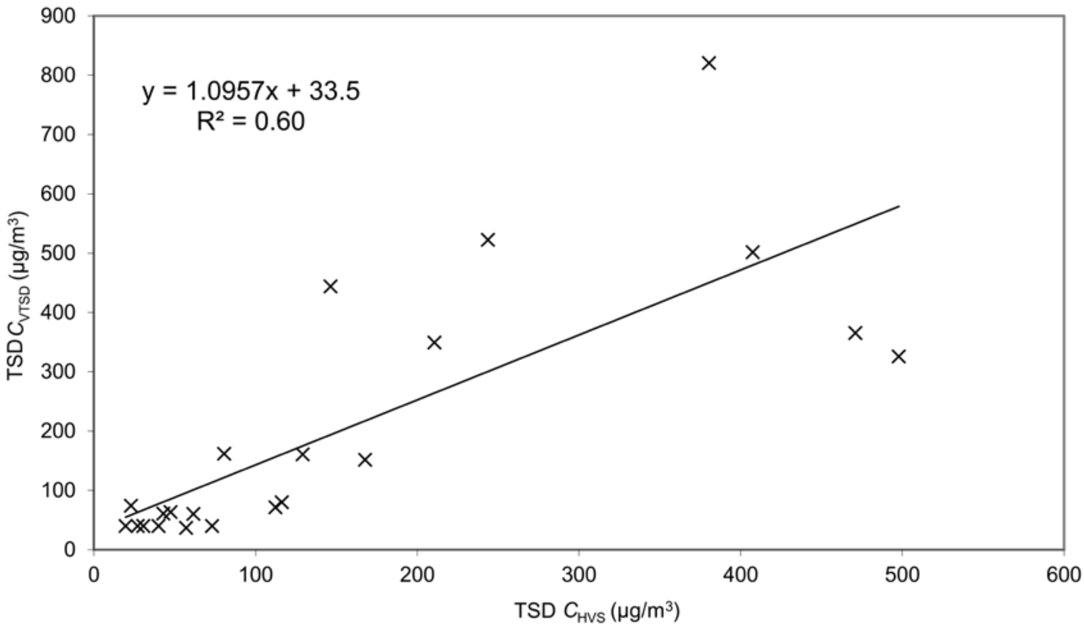
y = 1.0957x + 33.5
R² = 0.60
TSD C_VTSD (μg/m³)
TSD C_HVS (μg/m³)
0
100
200
300
400
500
600
700
800
900

Figure 3

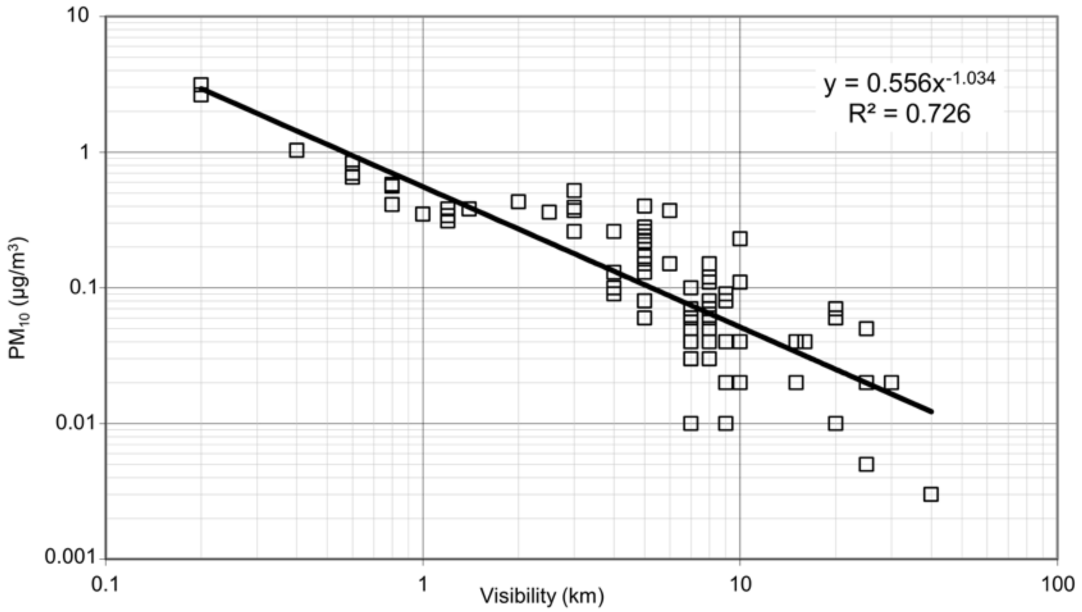
y = 0.556x-1.034
R² = 0.726
10
1
0.1
0.01
0.001
0.1
1
10
100
Visibility (km)
PM10 (µg/m3)

Figure 4

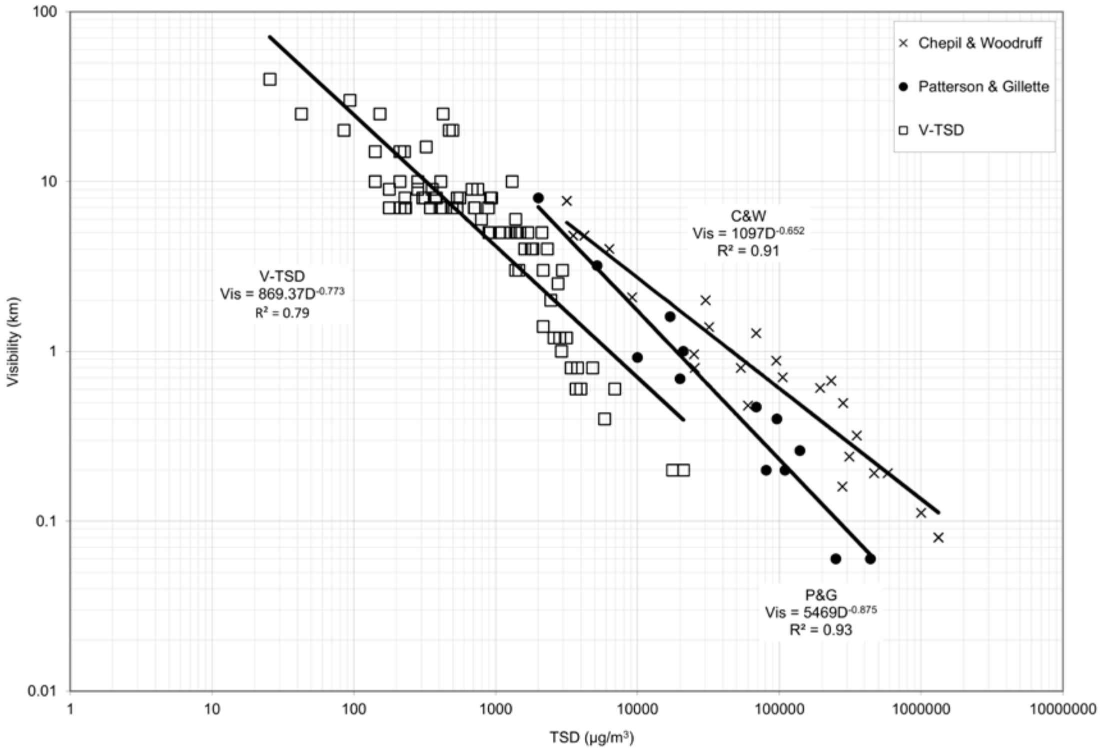

786

787 Figure 5